

# Effect of heating rate on the structure evolution of $(\text{K}_{0.5}\text{Na}_{0.5})\text{NbO}_3\text{--LiNbO}_3$ lead-free piezoelectric ceramics

Daijun Liu · Hongliang Du · Fusheng Tang · Fa Luo ·  
Dongmei Zhu · Wancheng Zhou

Received: 3 July 2007 / Accepted: 22 November 2007 / Published online: 11 December 2007  
© Springer Science + Business Media, LLC 2007

**Abstract** Lead-free piezoelectric ceramics  $(1-x)(\text{K}_{0.5}\text{Na}_{0.5})\text{NbO}_3\text{--}x\text{LiNbO}_3$  (abbreviated as KNLN) have been synthesized by traditional ceramics process. Effects of heating rate on the phase structure, microstructure evolution and piezoelectric properties of  $(1-x)(\text{K}_{0.5}\text{Na}_{0.5})\text{NbO}_3\text{--}x\text{LiNbO}_3$  were investigated. Results show that the heating rate has no effects on the phase structures. However, the fracture surface of the  $0.94(\text{K}_{0.5}\text{Na}_{0.5})\text{NbO}_3\text{--}0.06\text{LiNbO}_3$  ceramics transforms from intergranular fracture mode to a typical transgranular fracture mode with the increasing of the heating rate. This result is ascribed to the presence of agglomerates of grains which exhibit different sintering behavior at diverse heating rates. The  $0.94(\text{K}_{0.5}\text{Na}_{0.5})\text{NbO}_3\text{--}0.06\text{LiNbO}_3$  ceramic sintered at  $1080^\circ\text{C}$  with heating rate of  $5^\circ\text{C}/\text{min}$  shows the optimum piezoelectric properties ( $d_{33}=210\text{ pC/N}$ ,  $k_p=0.403$  and  $k_t=0.498$ ).

**Keywords** Lead-free piezoelectric ceramics ·  
 $(\text{K}_{0.5}\text{Na}_{0.5})\text{NbO}_3\text{--LiNbO}_3$  · Piezoelectric properties ·  
Microstructure evolution

## 1 Introduction

Lead-free piezoelectric ceramics have attracted considerable attention as new piezoelectric materials in place of  $\text{PbZrO}_3\text{--PbTiO}_3$  (PZT) based ceramics because of environmental protection reasons [1–4]. Recently, much attention

for lead-free piezoelectric ceramics has been paid to  $(\text{K}_{0.5}\text{Na}_{0.5})\text{NbO}_3$  (abbreviated as KNN)-based ceramics since Saito et al. had developed KNN-based textured ceramics with properties comparable to those of a basic, unmodified PZT ceramics [5–8]. It had been reported that pure KNN ceramics had high Curie temperature  $T_c$  of  $420^\circ\text{C}$ , high remnant polarization  $P_r$  of  $33\text{ }\mu\text{C}/\text{cm}^2$ , large piezoelectric constant  $d_{33}$  of  $160\text{ pC/N}$ , and high electro-mechanical coupling coefficients  $k_p$  of 45%. In addition, the low theoretical density of KNN can also be an advantage in transducers for underwater and medical imaging due to expected lower acoustical impedance. However, pure KNN ceramics are known to be difficult to densify fully by ordinary sintering method [9–11]. The hot press and spark plasma sintering were usually applied to prepare dense KNN ceramics. However, these approaches are unadapted to industrial production because of their rather high cost [12, 13]. On the other hand, comprehensive efforts have been made to find new systems based on KNN ceramics that can be sintered in a standard way and with improved properties, such as  $\text{KNN--BaTiO}_3$ ,  $\text{KNN--SrTiO}_3$ ,  $\text{KNN--LiTaO}_3$  and  $\text{KNN--LiNbO}_3$  [14–18]. Among these new systems, the  $(\text{K}_{0.5}\text{Na}_{0.5})\text{NbO}_3\text{--LiNbO}_3$  based ceramics were considered as an excellent candidate for lead-free piezoelectric ceramics because of high piezoelectric properties such as  $d_{33}=210\text{--}300\text{ pC/N}$  and high Curie temperature ( $450^\circ\text{C}$ ). Since lithium, potassium and sodium all belong to the alkali metal group, the new ternary  $\text{KNbO}_3\text{--NaNbO}_3\text{--LiNbO}_3$  system is more likely to have better prospects than that of the pure binary  $\text{KNbO}_3\text{--NaNbO}_3$  system. Guo et al. had reported the piezoelectric properties of KNLN ceramics [18, 19]. Until now, however, the effects of processing parameters on the phase structure and microstructure evolution were not reported. It is very beneficial to understand the structure evolution of the

D. Liu (✉) · H. Du · F. Tang · F. Luo · D. Zhu · W. Zhou  
State Key Laboratory of Solidification Processing,  
Northwestern Polytechnical University,  
Xi'an 710072, China  
e-mail: sunland1314@163.com

ceramics during sintering processing in detail because the properties of the ceramics have a close relationship with the structures.

Consequently, the purpose of this paper is to investigate the effects of processing condition on the structure evolution and piezoelectric properties of  $(1-x)(\text{K}_{0.5}\text{Na}_{0.5})\text{NbO}_3-x\text{LiNbO}_3$  ceramics and to provide an excellent promising candidate for lead-free piezoelectric ceramics.

## 2 Experiment

It is well known that the morphotropic phase boundary (MPB) plays a very important role in piezoelectric ceramics because the piezoelectric and dielectric properties show a maximum around the MPB [23, 24]. Guo and Kakimoto et al. had reported that the MPB of  $(1-x)(\text{K}_{0.5}\text{Na}_{0.5})\text{NbO}_3-x\text{LiNbO}_3$  existed at about 5–7 mol% of  $\text{LiNbO}_3$  by XRD and Raman scattering study, and the piezoelectric properties showed the maximum at 6 mol% of  $\text{LiNbO}_3$  [18–22]. Therefore,  $(1-x)(\text{K}_{0.5}\text{Na}_{0.5})\text{NbO}_3-x\text{LiNbO}_3$  ceramics ( $x=0\text{--}8$  mol%) were fabricated by traditional ceramics process.

Reagent-grade oxide and carbonate powders of  $\text{Li}_2\text{CO}_3$ ,  $\text{Na}_2\text{CO}_3$ ,  $\text{K}_2\text{CO}_3$  and  $\text{Nb}_2\text{O}_5$  were used as starting materials. Before being weighed, these powders were first separately dried in an oven at  $110^\circ\text{C}$  for 5 h. They were milled for 24 h using planetary milling with zirconia ball media and alcohol. After drying, the mixed powder was calcined in an alumina crucible at  $850^\circ\text{C}$  for 5 h. The calcined powders were ball milled again for 12 h, then dried and pressed into disks of 12 mm in diameter and 1.2 mm in thickness using PVA as a binder. After burning off PVA, the pellets were sintered at  $1080^\circ\text{C}$  [25, 26] with variable heating rates of 2, 3, 4, 5 and  $6^\circ\text{C}/\text{min}$ .

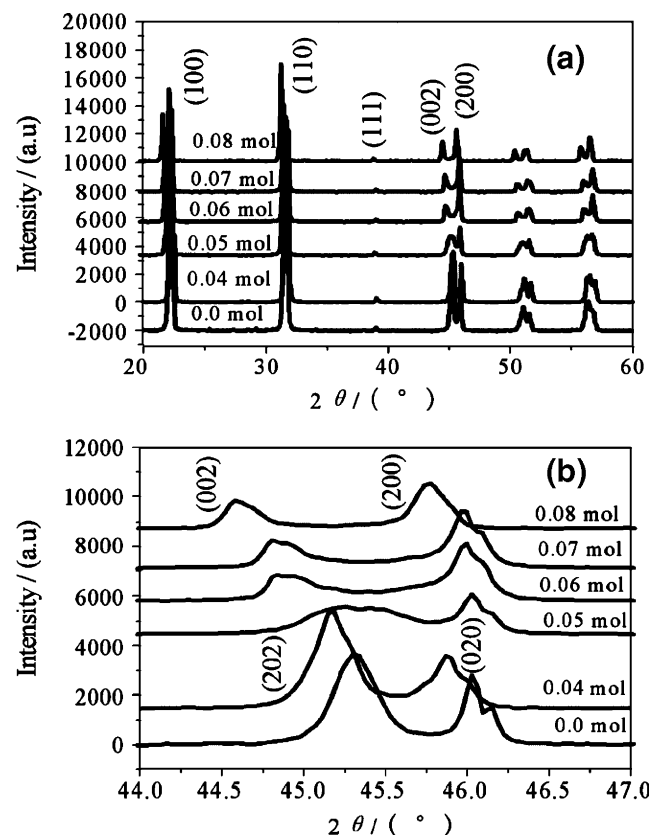
The bulk densities of sintered samples were measured by Archimedes method. The crystal structures were determined by XRD method (Philips X-Pert Diffractometer). Microstructure evolution of  $(1-x)(\text{K}_{0.5}\text{Na}_{0.5})\text{NbO}_3-x\text{LiNbO}_3$  was observed by scanning electron microscopy (SEM: Model JSM-6360 Japan). The average grain diameters were determined from the number of grains in the fixed area. For electrical characterization, silver electrodes were prepared on both sides of a disk and the samples were immersed in silicon oil and poled in 30 kv/cm field at  $120^\circ\text{C}$  for 30 min. The dielectric properties were determined using an Agilent 4294A precision impedance analyzer in the temperature range from 0 to  $550^\circ\text{C}$ . The Piezoelectric coefficient  $d_{33}$  was measured by a quasi-static meter (Model ZJ-3, Institute of Acoustics Academic Sinica). The electromechanical coupling factor  $k_p$  were determined by the resonance and antiresonance method according to IEEE standards using an impedance analyzer (Agilent 4294A).

## 3 Results and discussion

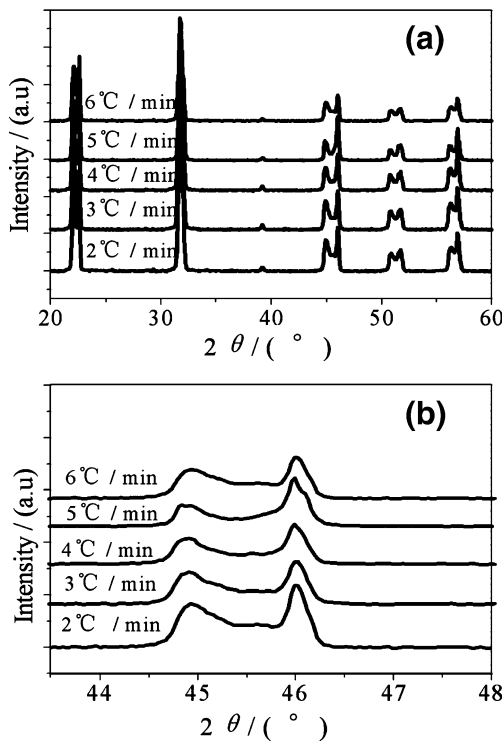
### 3.1 Phase analysis content

Figure 1(a) shows the XRD patterns of  $(1-x)(\text{K}_{0.5}\text{Na}_{0.5})\text{NbO}_3-x\text{LiNbO}_3$  ( $0\leq x\leq 0.08$ ) ceramics sintered at  $1080^\circ\text{C}$  with heating rate of  $5^\circ\text{C}/\text{min}$ . The phase structure in all samples is pure perovskite phase and no secondary phase could be identified. This result indicates that the  $\text{LiNbO}_3$  has diffused into the  $(\text{K}_{0.5}\text{Na}_{0.5})\text{NbO}_3$  lattice to form a new solid solution when the content of  $\text{LiNbO}_3 < 0.08$  mol. Figure 1(b) shows the XRD patterns of  $(1-x)(\text{K}_{0.5}\text{Na}_{0.5})\text{NbO}_3-x\text{LiNbO}_3$  ( $0\leq x\leq 0.08$ ) ceramics in the  $2\theta$  range of  $44\text{--}47^\circ$ . As shown in this figure, the phase structure of NKLN ceramics transformed from the splitting of (202)/(020) peaks to the splitting of (002)/(200) peaks at about  $45^\circ$  and the diffraction peaks shift to lower  $2\theta$  angles with the increasing of the content of  $\text{LiNbO}_3$ . It indicates that the phase structure changes with the amounts of  $\text{LiNbO}_3$ . The results are in agreement with the previously research reported by Guo YP et al. [19, 23].

Figure 2 shows the XRD patterns of  $0.94(\text{K}_{0.5}\text{Na}_{0.5})\text{NbO}_3-0.06\text{LiNbO}_3$  ceramics sintered at  $1080^\circ\text{C}$  with different heating rates. It can be seen that the diffraction



**Fig. 1** (a, b) XRD patterns of  $(1-x)(\text{K}_{0.5}\text{Na}_{0.5})\text{NbO}_3-x\text{LiNbO}_3$  ( $0\leq x\leq 0.08$ ) ceramics sintered at  $1080^\circ\text{C}$  for 2 h



**Fig. 2** (a, b) XRD patterns of  $0.94(K_{0.5}Na_{0.5})NbO_3-0.06LiNbO_3$  ceramics sintered at  $1080^\circ C$  with different heating rates

peaks of the KNLN ceramics do not change with the variation of heating rates.

These results indicate that the phase composition of KNLN is determined mainly by the contents of  $LiNbO_3$ .

**Fig. 3** SEM micrograph of the fracture surface of the  $0.94(K_{0.5}Na_{0.5})NbO_3-0.06LiNbO_3$  ceramics sintered at  $1080^\circ C$  with different heating rates: (a)  $2^\circ C/min$ ; (b)  $4^\circ C/min$ ; (c)  $5^\circ C/min$ ; (d)  $6^\circ C/min$

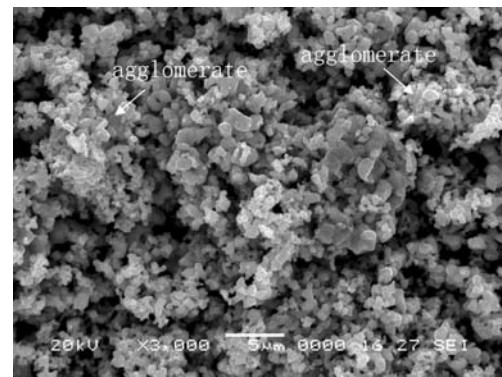
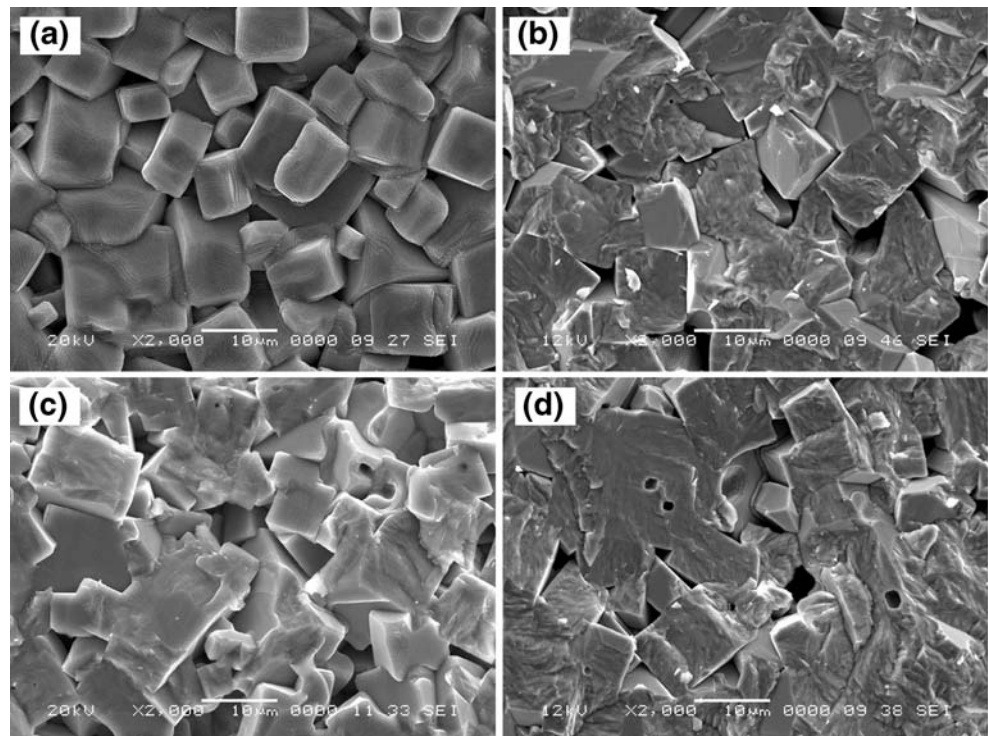


**Fig. 4** SEM micrograph of the  $0.94(K_{0.5}Na_{0.5})NbO_3-0.06LiNbO_3$  powders

The heating rate has no effects on the phase composition of the ceramics.

### 3.2 The microstructure evolution

Figure 3 shows the SEM micrograph of the fracture surface of the  $0.94(K_{0.5}Na_{0.5})NbO_3-0.06LiNbO_3$  ceramics sintered at  $1080^\circ C$  with different heating rates. As shown in Fig. 3(a), the fracture surface of the sample sintered at  $1080^\circ C$  with heating rate  $2^\circ C/min$  was intergranular fracture mode. The sample is easily broken due to weak grains bonding. The average grain size was about  $8\ \mu m$ , however, the fracture surface became typical of transgranular fracture when the heating rate was higher than  $4^\circ C/min$ . As shown in Fig. 3(b), the average grain size was

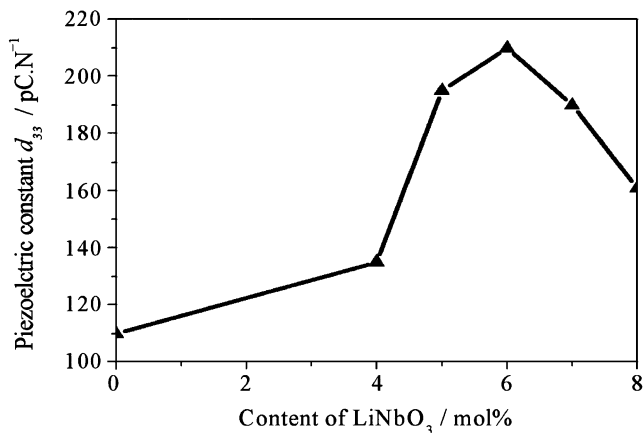


**Fig. 5** Piezoelectric constant  $d_{33}$  of  $(1-x)(K_{0.5}Na_{0.5})NbO_3-xLiNbO_3$  ceramics as a function of the  $LiNbO_3$  content

about 10  $\mu m$ . In the case of 5°C/min, indicated by Fig. 3(c), the microstructure was more homogeneous and dense, the grains were well formed and the grain boundary is clear. However, the microstructure became inhomogeneous and abnormal grain growth occurred when samples were sintered with heating rate 6°C/min. At the same time, distinct pores existed in the abnormal grains as seen in Fig. 3(d).

This result demonstrates that heating rate has a great influence on the microstructure evolution of KNLN ceramics. A possible reason is ascribed to the presence of agglomerates of KNLN powders, as shown in Fig. 4, which introduced a different sintering behavior at diverse heating rate.

As reported by E. R. Leite et al. [27, 28], the sintering of powders with agglomeration proceeds in two steps. The first step is the sintering between particles in agglomerates at low temperature, and the second one is the sintering between agglomerates at high temperature. However, in the condition of sufficiently high heating rate, both sintering steps of powders take place simultaneously.

In this study, densification of particles in agglomerates firstly proceeded and individual grains were formed at a rather low temperature due to a long exposure heating time when KNLN samples were sintered with a low heating rate (2°C/min). The finely crystallized grains in agglomerates were difficult to be sintered at high temperature, which induced weak bonding of grains and typical intergranular fracture

mode. Not fully crystallized particles in the agglomerates due to heating rate increase ( $\geq 4^\circ C/min$ ) could promote the sintering of agglomerates, which lead to stronger bonding of grains and typical transgranular fracture mode, as observed in Fig. 3. The fast movement of grain boundaries from higher heating rate ( $\geq 6^\circ C/min$ ) trapped gas in ceramics during the sintering. Therefore, the microstructure is inhomogeneous with abnormal grains and pores.

The piezoelectric properties of  $(1-x)(K_{0.5}Na_{0.5})NbO_3-xLiNbO_3$  ceramics were shown in Fig. 5. As it shows, the piezoelectric properties are greatly enhanced around the morphotropic phase boundary (MPB) at about 5–7 mol% of  $LiNbO_3$ . Thereinto, the  $0.94(K_{0.5}Na_{0.5})NbO_3-0.06LiNbO_3$  ceramics show the optimum piezoelectric properties with the  $d_{33}$  of 210 pC/N. Table 1 shows the properties of 0.94  $(K_{0.5}Na_{0.5})NbO_3-0.06LiNbO_3$  ceramics sintered at 1080°C with variable heating rates. It can be seen that the piezoelectric properties of the ceramics change with the variety of heating rate and the optimum properties of the ceramics reaches at about 5°C/min with bulk density and piezoelectric constant  $d_{33}$  of 4.337 g/m<sup>3</sup> and 210 pC/N, respectively.

The results indicate that the piezoelectric properties mainly depend on the content of  $LiNbO_3$  because of the presence of the phase mixture around MPB and the different microstructures of KNLN ceramics sintered at diverse heating rate lead eventually to a variation of the properties.

#### 4 Conclusions

The phase structure of  $(1-x)(K_{0.5}Na_{0.5})NbO_3-xLiNbO_3$  changes with the increasing contents of  $LiNbO_3$ . The orthorhombic and tetragonal phases co-exist when the content of  $LiNbO_3$  is in the range of 0.05–0.07 mol. The heating rate has no effects on the phase structure of  $(K_{0.5}Na_{0.5})NbO_3-LiNbO_3$  ceramics.

The heating rate has great effects on the microstructure evolution. The fracture surface of KNLN ceramics transforms from the intergranular fracture to a typical transgranular fracture with the increasing of heating rate. This result was ascribed to the presence of agglomerates of

**Table 1** The properties of  $0.94(K_{0.5}Na_{0.5})NbO_3-0.06LiNbO_3$  ceramics sintered at 1080°C with variable heating rates.

Heating rate	2°C/min	3°C/min	4°C/min	5°C/min	6°C/min	SPS (KNN) [29]
Bulk density (g/cm <sup>3</sup> )	4.236	4.255	4.297	4.337	4.222	4.45
Piezoelectric constant $d_{33}$ (pC/N)	182	180	200	210	194	148
Coupling coefficient $k_p$	0.35	0.36	0.389	0.403	0.37	0.35
Dielectric constant $\epsilon/\epsilon_0$	728	736	754	799	723	725
Dielectric loss $\tan \delta$	0.037	0.026	0.047	0.038	0.042	0.03

Dielectric properties were measured at 1 kHz.

KNLN grains which present different sintering behaviors at diverse heating rate.

The processing parameters have a great influence on the piezoelectric properties of the KNLN ceramics, too. The  $0.94(\text{K}_{0.5}\text{Na}_{0.5})\text{NbO}_3-0.06\text{LiNbO}_3$  ceramics sintered at  $1080^\circ\text{C}$  with heating rate of  $5^\circ\text{C}/\text{min}$  show optimum piezoelectric properties with the piezoelectric constant  $d_{33}$ , the coupling coefficient  $k_p$  and  $k_t$  of 210 pC/N, 0.403 and 0.498, respectively.

**Acknowledgments** This work was financially supported by the National Natural Science Foundation of China (Grant No. 10474077) and the Doctorate Foundation of Northwestern Polytechnical University (Grant No. CX200609).

## References

1. T. Abraham, J. Am. Ceram. Bull. 9, 45–47 (2000)
2. T. Takenaka, H. Nagata, J. Europ. Ceram. Soc. 25, 2693–2700 (2005)
3. W.W. Wolny, J. Europ. Ceram. Soc. 25, 1971–1976 (2005)
4. E. Ringgaard, T. Wurlitzer, J. Europ. Ceram. Soc. 25, 2701–2706 (2005)
5. Y. Saito, H. Takao, T. Tani, Nature 432, 84–87 (2004)
6. E. Cross, Nature 432, 24–25 (2004)
7. E. Hollenstein, M. Davis, D. Damjanovic, N. Setter, Appl. Phys. Lett. 87, 82905 (2005)
8. W. Chen, Y.M. Li, Q. Xu, J. Zhou, J. Electroceramics. 15, 229–235 (2005)
9. L. Egerton, D. M. Dillow, J. Am. Ceram. Soc. 42, 438–442 (1954)
10. R.E. Jeager, L. Egerton, J. Am. Ceram. Soc. 45, 208–213 (1962)
11. M.D. Marder, D. Damjanovic, N. Setter, J. Electroceramics. 13, 385–392 (2004)
12. G.H. Haertling, J. Am. Ceram. Soc. 50, 329–330 (1967)
13. R.P. Wang, R.J. Xie, T. Sekiya, Y. Shimojo, Y. Akimune, N. Hirosaki, M. Itoh, Jpn. J. Appl. Phys. 41, 7119–7122 (2002)
14. Y.T. Lu, X.M. Chen, D.Z. Jin, X. Hu, Mater. Res. Bull. 40, 1847–1855 (2005)
15. M. Kosec, V. Bobnar, M. Hrobar, J. Bernard, B. Malic, J. Holc, J. Mater. Res. 19, 1849–1854 (2004)
16. Y.P. Guo, K. Kakimoto, H. Ohsato, Mater. Lett. 59, 241–244 (2005)
17. M. Matsubara, T. Yamaguchi, K. Kikuta, S. Hirano, Jpn. J. Appl. Phys. 44, 6136–6142 (2005)
18. Y.P. Guo, K. Kakimoto, H. Ohsato, Appl. Phys. Lett. 85, 4121–4123 (2004)
19. K. Kakimoto, K. Akao, Y.P. Guo, H. Ohsato, Jpn. J. Appl. Phys. 44, 7064–7067 (2005)
20. T. Shrout, et al., J. Electroceram. 19, 111–124 (2007)
21. S. Zhang et al., J. Appl. Phys. 100, 104108 (2006)
22. Y. Dai, et al., Appl. Phys. Lett. 90, 262903 (2007)
23. R. Guo, L.E. Cross, S.-E. Park, B. Noheda, D.E. Cox, G. Shirane, Phys. Rev. Lett. 84, 5423–5426 (2000)
24. D.E. Cox, B. Noheda, G. Shirane, Y. Uesu, K. Fujishiro, Y. Yamada, Appl. Phys. Lett. 79, 400–402 (2001)
25. F. Tang, H. Du, Z. Li, et al., Trans. Nonferrous Met. Soc. China 16, s466–s469 (2006)
26. H.L. Du, F.S. Tang, D.J. Liu et al., Mater. Sci. Eng:B 136, 165–169 (2007)
27. E.R. Leite, M. Cerqueira, M.A.L. Nobre, E. Longo, J.A. Varela, J. Am. Ceram. Soc. 80, 2649–2652 (1997)
28. E.R. Leite, M.A.L. Nobre, M.D. Ribeiro, J. Mater. Sci. 33, 4791–4795 (1998)
29. B.P. Zhang, J.F. Li, K. Wang, et al., J. Am. Ceram. Soc. 89(5), 1605–1609 (2006)